JOURNAL OF MATERIALS SCIENCE **38** (2003) 119– 126

Cross-sectional structure of the secondary wall of wood fibers as affected by processing

J. FAHLÉN, L. SALMÉN*
STFI, Swedish Pulp and Paper Research Institute, Box 5604, SE-114 86 Stockholm, Sweden
E-mail: lennart.salmen@stfi.se

Understanding the arrangement of wood polymers within the fiber wall is important for understanding the mechanical properties of the fibers themselves. Due to their high load bearing ability, the arrangement of cellulose fibrils within the cell wall are of special interest. In this work AFM—Atomic Force Microscopy—in combination with image processing has been used to obtain more information about the arrangement of cellulose aggregates (fibrils) in the secondary cell wall layer of spruce wood. The effects of chemical processing on the arrangement of these cellulose aggregates were also studied. Enlargement of cellulose aggregates was found in the initial phase of the kraft cook. This increase in cellulose aggregate dimensions depended mostly on temperature for treatment temperatures above 140°C, regardless of the amount of alkali present. Although hemicelluloses are lost to various degrees under alkaline conditions, the increase in cellulose aggregate size was mainly related to thermally induced rearrangement of the cellulose molecules. The mean side length of cellulose aggregates was found to be around 18 nm in unprocessed wood and 23 nm in processed wood. The cellulose aggregates were assumed to be square shaped in cross section in both cases.

1. Introduction

Wood fibers are complex biocomposites built up of wood polymers whose complex composition give rise to a superior weight to strength ratio. After processing, however, structural defects in the fibers reduces their strength-bearing capacity. Reasons for this are found at both the fiber and ultrastructural levels. Knowledge pertaining to the ultrastructural changes occurring during processing is still limited.

The cell wall can schematically be viewed as composed of parallel cellulose aggregates within a matrix of lignin and hemicelluloses [1, 2]. The cellulose molecules are arranged into microfibrils approximately 3–4 nm in diameter, which in turn are aggregated into larger features called cellulose fibrils or cellulose aggregates 20–25 nm in diameter [3–5]. Mechanical investigations of the wood polymers show that there are strong interactions between the hemicelluloses, xylan and glucomannan, and the other wood polymers, cellulose and lignin. Studies of the softening behavior of glucomannan and xylan suggest that xylan is more associated with lignin while the glucomannan is more associated with cellulose [6]. This has also been supported by spectroscopic studies using the so-called dynamic FTIR [7]. Such an interaction is also in accordance with the proposal of Fengel, that some of the hemicelluloses are incorporated within the cellulose aggregates [5].

On a larger scale it is rather clear that the cell wall is organized in a lamella arrangement of cellulose aggregates and matrix material [1, 8–10]. There is still some disagreement as to whether the lamella structure has a concentric [10–13] or a radial [14] orientation.

In chemical pulping the aim of the pulp liquor is to delignify the wood, in particular the middle lamella, to make it possible both to separate the individual fibers and produce a strong and durable fiber product. The pulping liquor promotes degradation and dissolution of the lignin, although at the same time the polysaccharides are attacked. The chemical interaction of the cell wall components with kraft pulp liquor, which consists of sodium hydroxide and sodium sulfide or more correctly hydroxide and hydrosulfide ions, is well known. On the other hand, understanding of the effects of chemical processing and especially the effects of the pulp liquor on cell wall ultrastructure is still limited.

This study used atomic force microscopy (AFM) to examine closely the morphological arrangement of cellulose aggregates within the secondary wall of wood fibers, and to examine the changes occurring at this level due to processing under conditions equivalent to those in an ordinary kraft cook. The morphological changes were then related to the chemical structure of the processed wood by looking at changes in its chemical composition.

*Author to whom all correspondence should be addressed.

2. Materials

From fresh undried Norway spruce (*Picea abies*) samples, 40 mm in the longitudinal direction and one annual ring in the transverse and radial direction were prepared. Each of these rods was further cut into smaller pieces about 8 mm long. The samples were thereafter cut in two halves in order to obtain two adjacent samples sharing a face: one sample was pulped and the other was kept as a control. This procedure was adopted to get comparable surfaces for the AFM investigations, and five sets of such samples were made. The unprocessed control samples were labeled 1w to 5w respectively. The corresponding experimental samples, labeled 1p to 5p, were processed using an ordinary kraft cook sequence, with a start up cycle of 100 min from 20°C to 170°C (Fig. 1). The wood to water ratio was 1 : 4, the effective alkali was 19%, and the sulfidity was 40%. After processing the samples were kept wet to prevent changes in the ultrastructure due to drying. All samples were then rapidly frozen in liquid nitrogen, freeze-dried, embedded in epoxy-resin (TAAB 812), and cut into 0.5 μm thick cross sections using a rotary microtome (Leica Jung RM 2065). The cross sections were placed on round object glasses approximately 1 cm in diameter.

To investigate the specific effects of temperature and alkali in the kraft cook, five additional wood pieces were prepared in the way described above. These unprocessed control samples are referred to as 6w to 10w. The corresponding experimental samples of the rods, 6p to 10p, were treated in water for 30 minutes at 50°C, 100°C, or 150°C. Alternatively the samples were treated in an alkaline environment (effective alkali 100 percent) at room temperature for 30 minutes or at 150°C for 30 minutes (Table I). The relative composition of polysaccharides in the wood chips after this treatment is shown in Table II. The experimental cross sections were then prepared in the same way as described above for the kraft cook samples.

TABLE I Processing conditions for the part of the samples that were processed in the study of the effect of temperature and alkalinity on the cellulose aggregate dimensions

Sample number	Final temperature (°C)	Processing time (min)	pH
6p	50	120	Deionized water
7p	100	120	Deionized water
8p	150	120	Deionized water
9p	50	120	Effective alkali 100%
10p	150	120	Effective alkali 100%

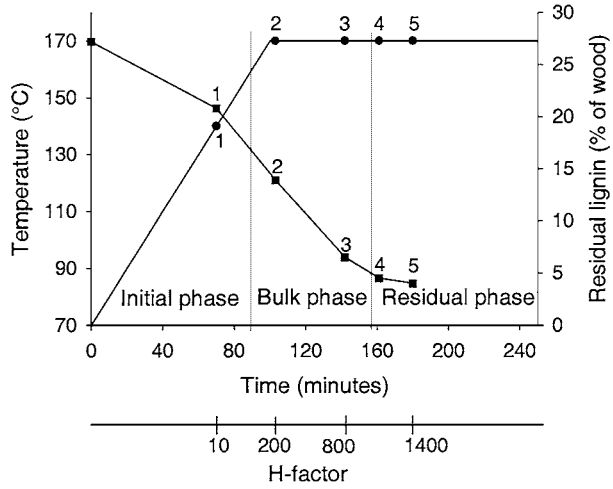

Figure 1 Processing conditions for the samples that were processed in a kraft cook sequence; circles represent processing temperature and squares represent lignin content of wood.

3. Methods

The embedded wood cross sections were examined with AFM using TappingMode™. A NanoScope® Illa Dimension™ 3000 with standard tapping mode probes was used. The specimens were scanned using a tip with a radius about 10 nanometers. The length of the cantilever was 125 μm, the spring constant was 42 N/m, and the resonant frequency was 330 kHz. The samples were scanned at ambient temperature and humidity. Images were taken in both height mode, in which the deflection of the cantilever is directly used to measure the z position, and in phase mode, where the phase lag of the cantilever is used to determine differences in material stiffness.

For each sample a few fibers in both the early- and latewood were randomly chosen and analyzed. For each fiber two images from independent, positions were examined.

Image processing software (called IMP), developed at the Center for Image Analysis in Uppsala [15] and based on the watershed algorithm [15, 16], was used for evaluation of the AFM images. After detection by the software, each individual aggregate area was calculated in pixels, which then was transformed to nm. From the mean area values of the aggregates their widths can

TABLE II Relative composition, percent, of polysaccharides in the processed wood chips

Samples	6p	7p	8p	9p	10p
Processing conditions	50°C Deionized water	100°C Deionized water	150°C Deionized water	50°C Effective alkali 100%	150°C Effective alkali 100%
Polysaccharides					
Arabinose	1.7	1.7	1.7	1.7	1.6
Xylose	8.1	8.1	8.0	7.0	7.0
Mannose	18.3	18.0	18.1	13.9	12.3
Galactose	4.4	4.4	4.0	3.5	2.7
Glucose	67.4	67.8	68.2	73.9	76.4
Total	100	100	100	100	100

be calculated, assuming a square cross-section for the cellulose aggregates.

The shape of the tip influences the apparent width and height of the cell wall features, with low areas appearing smaller and high features appearing larger. The enlargement of the AFM probe is hard to calculate with high accuracy because several factors are involved in the result, factors such as the tip radius, the radius of the features imaged, the depth of the valleys between individual objects. A rough estimate of the enlargement effect is however possible. Knowing the angle of the tip (10°) and an average value for individual cellulose aggregate height (8–14 nm) from the AFM software's roughness function, using ordinary triangle trigonometry the enlargement effect was estimated to be 2 ± 1 nm (see Fig. 2).

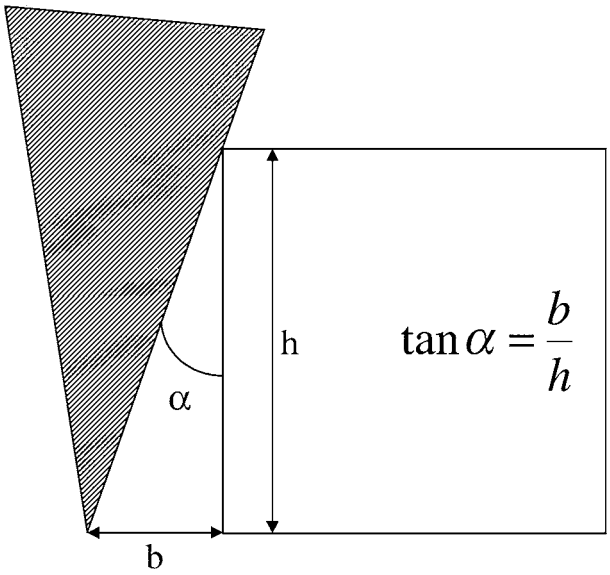

Figure 2 An illustration of how the enlargement (b) effect is calculated.

4. Results

Fig. 3 shows a cross section of a native latewood spruce fiber taken in the AFM height mode. In this image lumen and the thick fiber wall are clearly visible. The different layers of the cell wall, such as the middle lamella, the primary wall, and the secondary wall (with the S_1, S_2 and S_3 layers), are also evident as is the concentric lamella arrangement in these walls. It is obvious that the direction of the lamella follows the tangential curvature of the cell wall. Fig. 4 shows an image of part of the S_2 layer in a wood fiber from sample 1w taken in the AFM phase imaging mode. In such a phase contrast image, lighter areas correspond to regions of higher stiffness. These areas also correspond to portions that are higher than the surrounding regions. These lighter areas are likely to be associated with cellulose aggregates, which are known to be stiffer than the hemicellulose-lignin

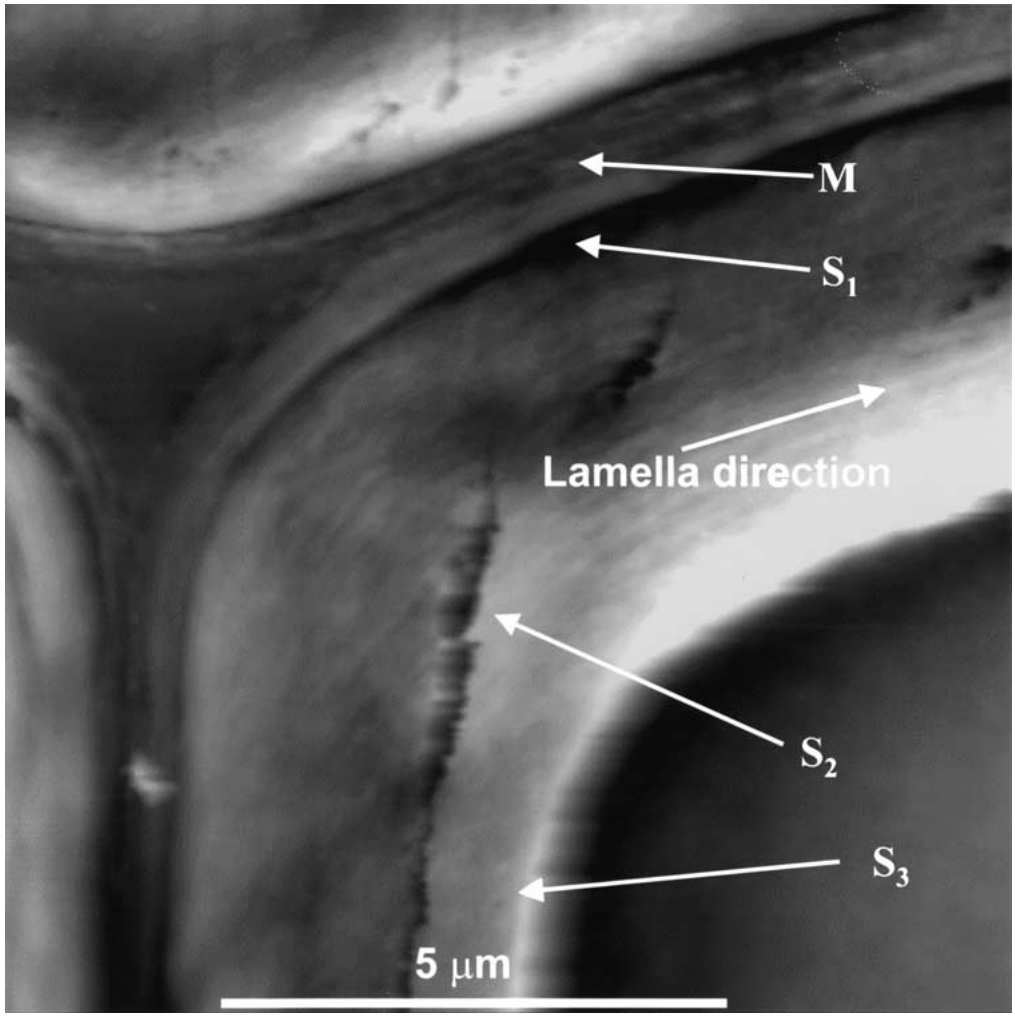

Figure 3 An AFM image of a native spruce latewood fiber (height mode).

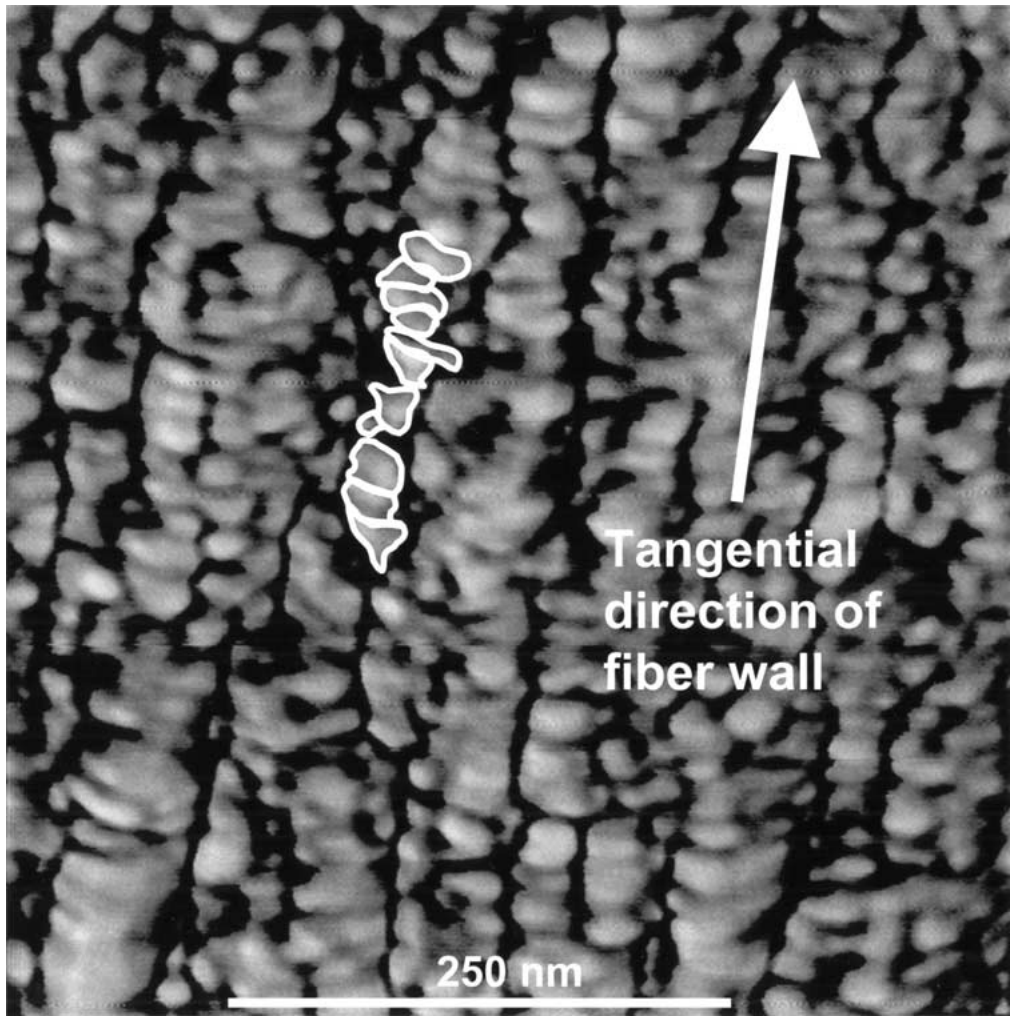

Figure 4 Part of the S_2 layer of a native spruce wood fiber, sample 1w. The individual cellulose aggregates can be seen (phase mode) and a few of them are marked for visualization.

matrix [17]. The sizes of these lighter areas range from approximately 10 to 30 nm, of the same order of size as expected for cellulose aggregates [5]. Regularity is also evident in the micrograph, which corresponds with the tangential directions of the fiber wall and could be interpreted as lignin lamellation, where the lignin is the dark areas in between the rows built up of cellulose aggregates.

From cuts made in two different directions it was apparent that the cuting itself had no influence on the structure examined.

Fig. 5 shows an AFM phase image of the S_2 layer of sample 1p, corresponding to the initial phase of a kraft cook with respect to lignin extraction [18–21]. Individual cellulose aggregates are visible in this micrograph; although it sometimes appears as if several aggregates a grouped in a row. In both Figs 4 and 5 example of individual cellulose aggregates are indicated. Visual comparison of the two images (Figs 4 and 5) gives the impression that the cellulose aggregates are larger in the processed sample (1p) than in the control sample (1w). This phenomenon appeared in each of the sample sets and suggests that enlargement of the cellulose aggregates had already occurred in the initial phase of the kraft cooking process.

To study the influence of kraft cooking variables on the enlargement of cellulose aggregates, tests at different temperatures and alkalinity were performed according to Table I. Fig. 6 shows an AFM phase mode image of part of the secondary cell wall layer of sample 10p, a wood sample heated to 150°C at very high alkalinity. The individual cellulose aggregates are clearly visible and were found to be larger than those in the corresponding control sample (Fig. 4). Enlargement of the cellulose aggregates was only found in samples 8p and 10p, which were processed at high temperatures (150°C). Samples treated at lower temperatures, even at high alkalinity, revealed no such enlargement. This indicates that the enlargement effect is primarily related to the high temperature in the kraft cook, although some hemicelluloses were dissolved in samples treated at lower temperatures (Table II).

Fig. 7 shows an example of the way in which the image processing software (IMP) detected and indicated the individual cellulose aggregates by circling them. From the data provided by the image processing software, the mean sizes of the cellulose aggregates for wood and the differently processed samples were calculated (Table III). The mean size was larger for the processed than for the unprocessed samples, in line with the appearance of the images. Table III shows the mean sizes determined for the various samples. These sizes are in line with the values for cellulose aggregates obtained by other methods [22, 23]. Care must,

TABLE III Cellulose aggregate size in both wood and processed samples

Wood sample	Aggregate size (nm)	Processed sample	Aggregate size (nm)	
			Enlarged	Unaffected
1w	17.3	1p	23.5	
2w	19.9	2p	23.8	
3w	19.6	3p	23.0	
4w	18.3	4p	21.8	
5w	17.4	5p	21.5	
6w	18.0	6p		18.2
7w	17.3	7p		17.8
8w	18.3	8p	22.7	
9w	18.0	9p		18.3
10w	18.7	10p	23.8	
Mean value for all wood samples	18.3	Mean value	22.8	18.1
Standard deviation for all wood samples	0.9	Standard deviation	0.8	0.2

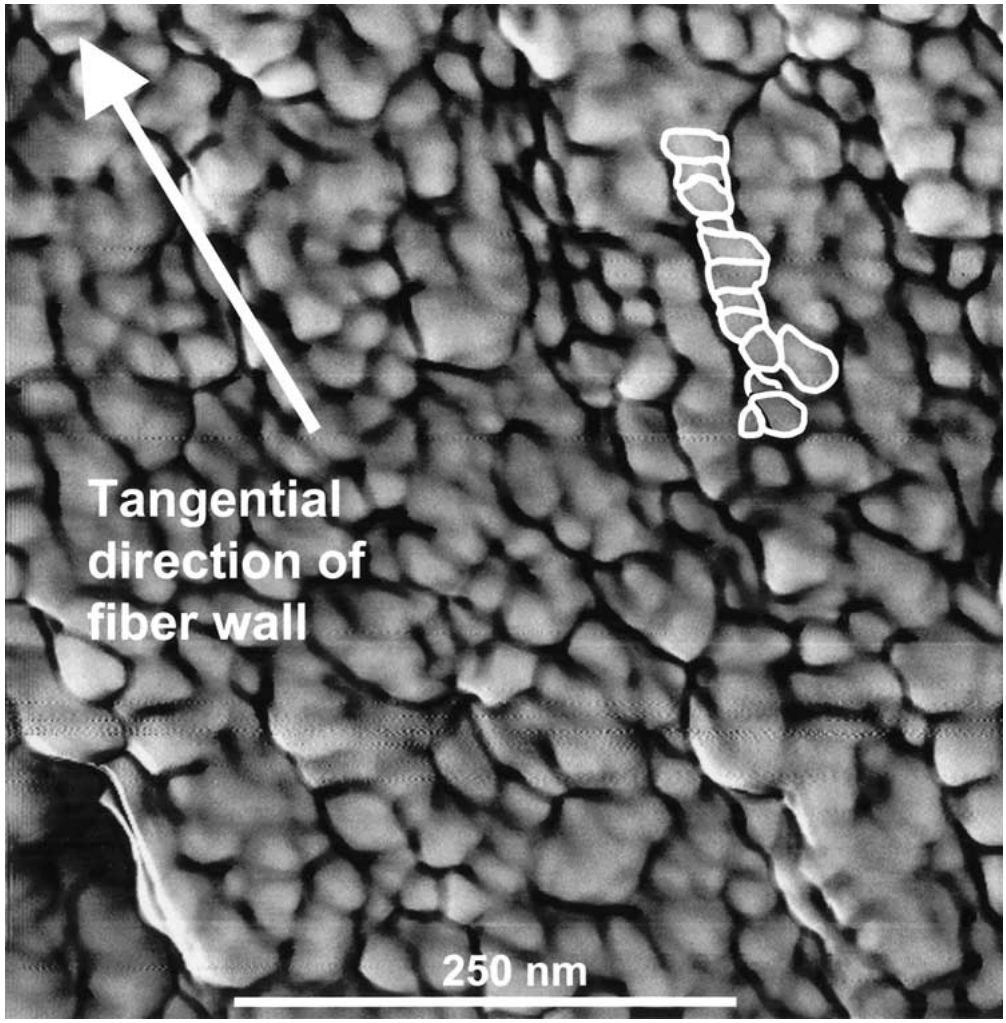

Figure 5 Part of the S_2 layer of a processed spruce wood fiber, sample 1p (phase mode). The individual cellulose aggregates can be seen, a few of them are marked for visualization, and are larger than those in Fig. 1.

however, be taken when calculating the apparent width and height of objects measured by AFM. The slightly higher values for the size of the cellulose aggregates determined by AFM in Table III, as compared with the results obtained using NMR [22] and SEM [23], are probably due to the enlargement effect of the AFM probe, an effect which adds about 2 nm to the values. A relatively large proportion of the cellulose aggregates perceived in the images are smaller than 15 nm. This probably stems from the fact that the image processing program detects all the aggregates, including those cut off by the image frame.

The distribution of cellulose aggregate sizes in the various samples was calculated assuming square cross sections for the cellulose aggregates. This assumption was adopted for comparison based on the model ideas of previous researchers [5, 22, 23]. The comparison of the distribution of mean values for the unprocessed and for the processed samples (Fig. 8) shows that in the processed samples a larger portion of the aggregates

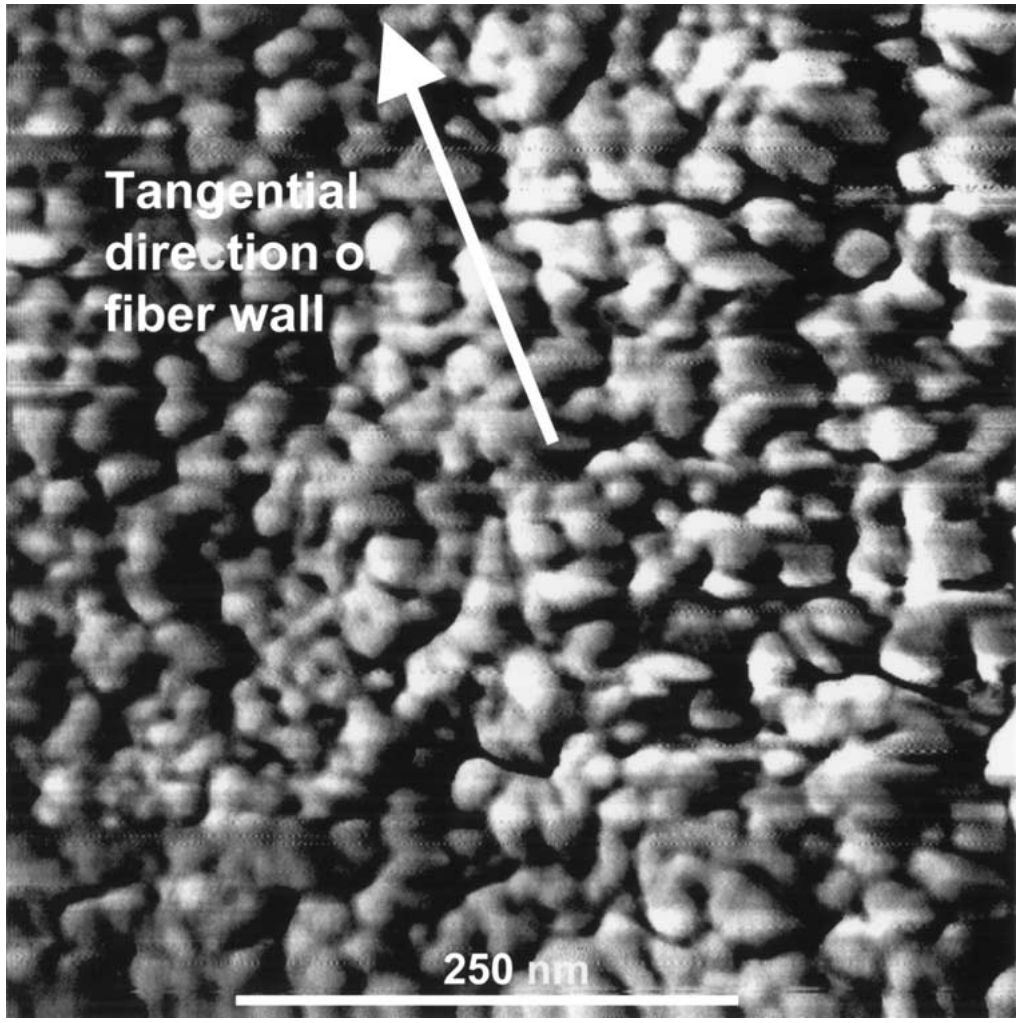

Figure 6 Part of the S_2 layer in a processed spruce wood fiber, sample 10p (phase mode). The individual cellulose aggregates can be seen and are larger than those in Fig. 1.

are larger than in the unprocessed wood samples. This confirms the perception gained from the image, namely that smaller aggregates aggregate to form larger ones during processing.

5. Discussion

A number of studies have suggested that the mean size of the cross sections of the cellulose aggregates (fibrils) are of the order of 15–25 nm [5, 22–24] assuming a square cross section for an individual cellulose aggregate. This study supports such findings, i.e., that the wood cell wall comprises cellulose aggregates which are embedded in a matrix of lignin and hemicelluloses. The individual aggregates have irregular forms but could on the average be presented as square shaped for comparison with other studies. The broad distribution of aggregate sizes could reflect the fact that they are an assembly of different numbers of cellulose microfibrils. Also, incorporation of approximately 30% of the total amount of hemicelluloses inside the cellulose aggregates could make them less well-defined [5]. This fact probably also implies that the aggregates are slightly larger than if they were only composed of cellulose molecules. This fact also makes the space between cellulose aggregates smaller than if none of the hemicelluloses were present inside the aggregates, as evidenced by the distance of only 4 nm between the aggregates seen in Figs 4–6.

The varying size of the aggregates accords well with the three-dimensional structure of cellulose fibrils proposed by Boyd [25]. If the enlargement effect were due to the combination of two neighboring cellulose aggregates, this new structure should have a diameter in the range of 40 nm. However this is not the case, and the rather small, 4–5 nm enlargement can be explained by the three-dimensional model proposed by Boyd and Foster [26], featuring microfibril bridges between adjacent cellulose aggregates. These microfibril bridges are likely to associate with one of the aggregates and form a structure 4–5 nm larger, which fits well with the experimental values found in Table III. These values for cellulose aggregates size vary greatly between different samples (Table III). This could be due to a large natural variability in structure between the individual wood fibers within an annual ring, as apparent from other fiber properties [27].

Hattula [28] has shown that under hydrothermal conditions wood cellulose changes its ultrastructure by means of two opposite mechanisms, crystallization and disordering. Under milder conditions, from 130°C to 175°C, crystallization of cellulose is dominant, while at higher temperatures cellulose is disordered [28]. During the kraft cook the temperature reaches 130°C in less

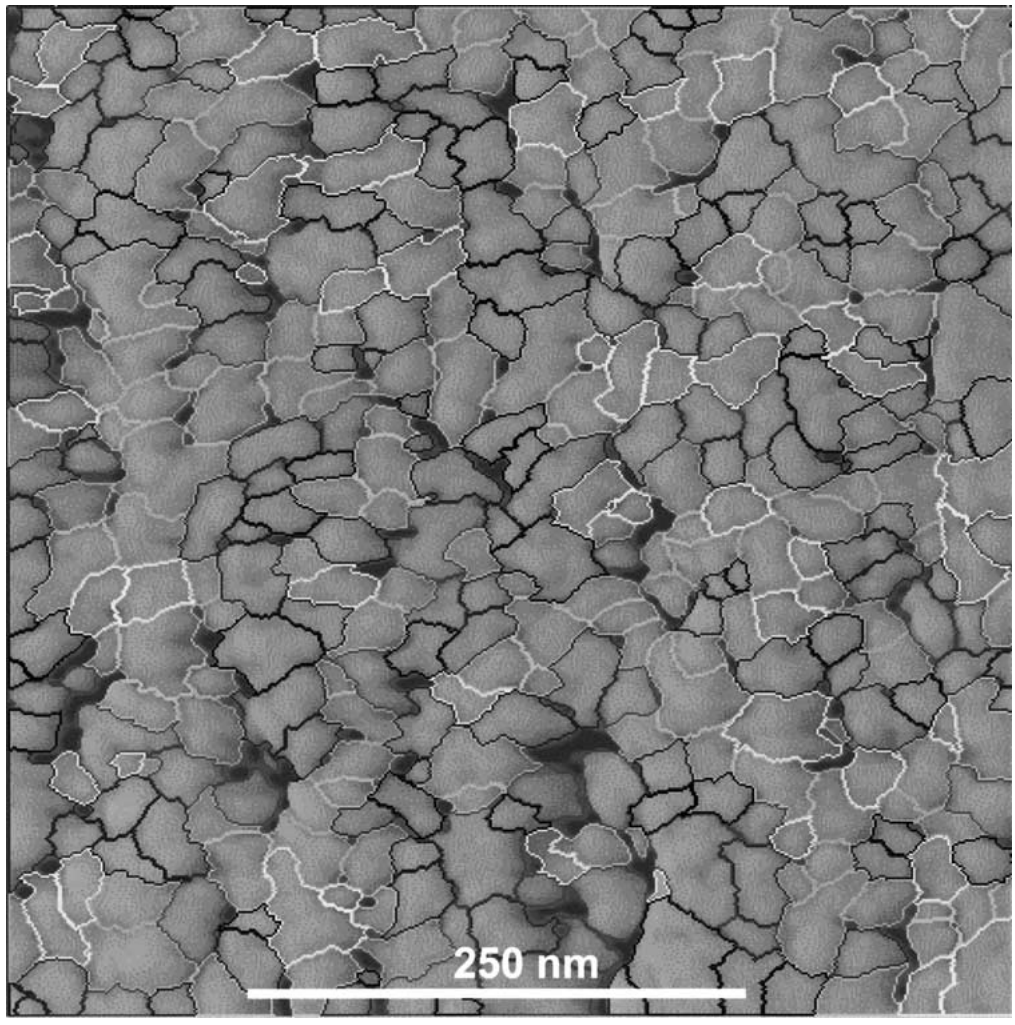

Figure 7 The marking of the individual cellulose aggregates by the image-processing program, sample 10p.

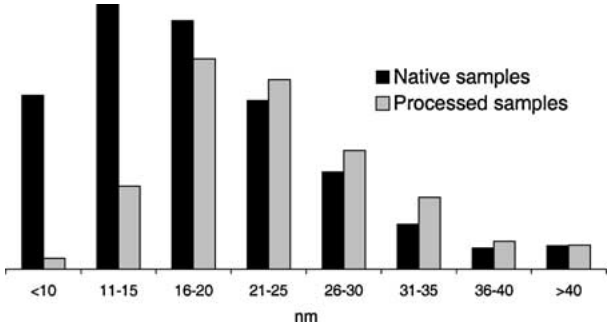

Figure 8 The size distribution of cellulose aggregates in unprocessed and processed spruce wood.

than one hour, which should favor crystallization of cellulose and thus contribute to the enlargement of cellulose aggregates. During kraft pulping and processing of spruce wood at a temperature above 140°C, dissolution of hemicelluloses also occurs (Table II). Also, part of the lignin is removed from the cell wall during these conditions [29]. The high alkalinity and the increased temperature during the cook also affect the physical properties of the lignin.

The softening temperature for the amorphous wood polymers is very high in the dry state, ranging between 180°C and 250°C [30]. In the water-saturated state there is a pronounced lowering of the softening temperature for wood. Spruce wood in the water-saturated state softens at about 90°C [31], a behavior assigned mainly to the lignin [30–32]. Thus under kraft pulping conditions the native lignin will have substantially increased movement; this is expected to increase the possibility of two adjacent cellulose microfibril surfaces coming into close contact and associating to form a larger unit. Although the kraft cook is accompanied by hemicellulose dissolution (mostly glucomannan), which could be assumed to promote association, the same dissolution occurs under alkali treatment at low temperature (compare sample 9p in Tables II and III) without enlargement of the aggregates. It is suggested that it is in fact that the lignin network is less constrained at the high temperatures, which is the prerequisite for achieving cellulose aggregate enlargement.

Synthetic polymers have large length-to-width ratios and their equilibrium crystal shapes can be calculated from the surface free energies by searching for energy minimums. When comparing such theoretical values with experimental ones it can be concluded that such synthetic polymer crystals are not in equilibrium. When given enough "thermal stimulation," synthetic polymer crystals with such unfavorable length-to-width ratios are expected to thicken or rearrange, to achieve a more stable crystal shape [33]. This phenomenon should also occur with cellulose crystals because they also have a large, unfavorable length-to-width ratio and

a less-ordered structure. The amorphous transitions for semicrystalline polymers are to a large extent dependent on the crystallinity; crystallites will broaden the transition regions for the less ordered form [34]. Cellulose has some weak transitions between 0°C and 225°C that could indicate the possibility of rearrangement given enough "thermal stimulation" [35]. Such rearrangement could initiate enlargement of the cellulose crystals and thus an enlargement of the cellulose aggregates. In the case of thermomechanical pulps (TMP) treated with both water and heat, an increase in the crystalline structure of cellulose was also found for temperatures over 130°C [28].

The results obtained suggest that temperature is the single most important parameter for cellulose aggregate enlargement. This conclusion is based on the observations that enlargement only appeared after treatment at temperatures above 140°C, and that no enlargement was observed after treatments with alkali at room temperature.

6. Conclusions

Atomic force micrographs of cross-sections of native spruce wood fibers have shown a structure of cellulose aggregates ranging from 15 to 25 nm per side assuming a square cross section. At high temperatures over 140° in a kraft cook, enlargement of cellulose aggregates occurs. The increased temperature apparently provides the matrix polymers enough energy to soften and gives the cellulose enough mobility to rearrange; enlargement of the cellulose aggregates thus takes place. The mean sizes for the cellulose aggregates showed a broad distribution both for unprocessed and processed spruce wood, with a shift of the mean values from 11 to 20 nm for unprocessed wood, and from 16 to 25 nm for processed wood.

Acknowledgement

This work was carried out with the support of the Wood Ultrastructure Research Center (WURC). The authors wish to thank the following for their valuable assistance: Ms. AnnCatrin Hagberg, STFI, for help with sample preparation; Ms. Carolina Wählby, M.Sc., at the Center for Image analysis in Uppsala, for help with the image processing software; Mr. Erik Petrini, ACREO AB, for help with the AFM equipment; and Professors Ulf Gedde and Ants Teder for their valuable advice and comments.

References

1. N. TERASHIMA, K. FUKUSHIMA, L.-F. HE and K. TAKABE, in "Forage Cell Wall Structure and Digestibility," edited by H. G. Jung, D. R. Buxton, R. D. Hatfield and J. Ralph (American Society of Agronomy, Madison, 1993) p. 247.
2. D. H. PAGE, *Wood and Fiber* **7** (1976) 246.
3. K. WICKHOLM, P. T. LARSSON and T. IVERSEN, *Carbohydrate Research* **312** (1998) 123.
4. P. T. LARSSON, K. WICKHOLM and T. IVERSEN, *ibid.* **302** (1997) 19.
5. D. FENGEL, *Tappi* **53** (1970) 497.
6. L. SALMÉN and A.-M. OLSSON, *Journal of Pulp and Paper Science* **24** (1998) 99.
7. M. ÅKERHOLM and L. SALMÉN, *Polymer* **42** (2001) 963.
8. H. ABE, J. OHTANI and K. FUKUZAWA, *IAWA* **12** (1991) 431.
9. Y. KATAOKA, H. SAIKI and M. FUJITA, *Mokuzai Gakkaishi* **38** (1992) 327.
10. K. RUEL, F. BARNOUD and D. A. I. GORING, *Wood Science and Technology* **12** (1978) 287.
11. A. J. KERR and D. A. GORING, *Cellulose Chemistry and Technology* **9** (1975) 536.
12. A. STAMM and W. SMITH, *Wood Science and Technology* **3** (1969) 301.
13. J. E. STONE and A. M. SCALLAN, *Cellulose Chemistry and Technology* **2** (1968) 343.
14. J. SELL and T. ZIMMERMANN, *Holz als Roh- und Werkstoff* **51** (1993) 384.
15. C. WÄHLBY, F. ERLANDSSON, K. NYBERG, J. LINDBLAD, A. ZETTERBERG and E. BENGTSSON, in Proceedings of 12th Scandinavian Conference on Image Analysis, Bergen, Norway (2001).
16. L. VINCENT and P. SOILLE, *Transactions on Pattern Analysis and Machine Intelligence* **13** (1991) 583.
17. R. E. MARK, "Cell Wall Mechanics of Tracheids" (Yale University Press, London, 1967).
18. S. LÉMON and A. TEDER, *Svensk Papperstidning* **76** (1973) 407.
19. T. D. KLEINERT, *Tappi Journal* **49** (1966) 53.
20. P. J. KLEPPE, *ibid.* **53** (1970) 35.
21. H. D. WILDER and E. J. DALESKI, *ibid.* **48** (1965) 293.
22. E.-L. HULT, P. T. LARSSON and T. IVERSEN, *Polymer* **42** (2001) 3309.
23. I. DUCHESNE and G. DANIEL, *Nordic Pulp & Paper Research Journal* **15** (2000) 54.
24. H. F. JAKOB, D. FENGEL, S. E. TSCHEGG and P. FRATZL, *Macromolecules* **28** (1995) 8782.
25. J. D. BOYD, in "New Perspective in Wood Anatomy," edited by P. Baas (Martinus Nijhoff/Dr W Junk, La Hague, 1982) p. 171.
26. J. D. BOYD and R. C. FOSTER, *Canadian Journal of Botany* **53** (1975) 2687.
27. A. BERGANDER, Doctoral thesis, Royal Institute of Technology (2001).
28. T. HATTULA, Doctoral thesis, University of Helsinki (1985).
29. A. R. PROCTER, W. Q. YEAN and D. A. I. GORING, *Pulp and Paper Magazine of Canada* (1967) T445.
30. E. BACK and L. SALMÉN, *Tappi* **65** (1982) 107.
31. A.-M. OLSSON and L. SALMÉN, *Nordic Pulp and Paper Research Journal* **12** (1997) 140.
32. G. IRVINE, *Tappi* **67** (1984) 118.
33. U. W. GEDDE, "Polymer Physics" (Kluwer Academic Publishers, Dordrecht, 1996).
34. L. E. NIELSEN and R. F. LANDEL, "Mechanical Properties of Polymers and Composites" (Marcel Dekker, New York, 1994).
35. C. KLASON and J. KUBÁT, *Svensk Papperstidning* **79** (1976) 494.

Received 11 July 2001
and accepted 9 April 2002